ECCTD'01 - European Conference on Circuit Theory and Design, August 28-31, 2001, Espoo, Finland

Symbolic Distortion Analysis of Analog Integrated Circuits

Wim Verhaegen* and Georges Gielen*

Abstract — **A technique for generating symbolic expressions for the distortion in weakly nonlinear analog integrated circuits is presented. This technique uses some acceptable assumptions to reduce the task of analyzing the nonlinear circuit to a repeated analysis of derived linear circuits. This repetitive algorithm has been implemented and it is demonstrated on an example circuit.**

1 Introduction

In the analysis of analog integrated circuits, distortion and intermodulation are important factors. Either they are unwanted, as is the case in linear building blocks like opamps, or they are explicitly wanted to obtain a signal shifted in frequency, as is the case with mixers. Distortion and intermodulation need to be assessed accurately in both cases.

Classical numerical simulation techniques using iterative algorithms for solving the differential equations are slow and inaccurate due to the large difference between the time constants normally present in the circuits of interest. Several numerical methods have been developed to overcome this problem, e.g. the harmonic balance technique [1], multitime analysis [2] and the use of describing functions in circuits with feedback [3]. However, the numerical nature of these techniques implies that no symbolic results can be derived, so that re-use of results — in the form of design equations — is not possible.

An analysis technique that does yield symbolic results is described in this paper. Based on a set of assumptions, the analysis of a weakly nonlinear circuit is reduced to a number of analyses of linear circuits. A linear symbolic analysis core is used for these individual analysis steps, and its results are combined and manipulated to get a closed–form symbolic end result. This result can be used as a design equation, or the impact of the circuit nonlinearities on distortion and intermodulation can be derived from it.

Before explaining this technique, it is to be noted that similar approaches have been followed in the past to obtain symbolic expressions for the distortion in specific classes of circuits. E.g. the distortion in sampling mixers is analyzed in [4], and a method for analyzing the distortion in analog building blocks is presented in [5]. All symbolic approaches are intrinsically limited someway, and these publications are no exceptions. The scope of the algorithm presented in this paper is limited to weakly nonlinear circuits. This means that the circuit characteristics are nonlinear in a smooth way, implying that higher–order contributions are always smaller than lower–order ones, and that the applied signals are small.

The basic terminology used is explained in section 2, followed by a brief explanation of the algorithm in section 3. The implementation is demonstrated in section 4, and the conclusions are presented in section 5.

2 Terminology

The following terms are used in this paper:

- An *n–dimensional conductance* is a conductance with n controlling branch voltages. When analyzing analog integrated circuits, n equals 3 at most. The corresponding branch voltages are denoted as v_i, v_j and v_k in this paper.
- A nonlinear current is described using its DC component and the derivatives to the controlling branch voltages. The derivatives up to order 3 are described by *nonlinearity coefficients*. E.g. the q'th–order nonlinearity coefficient $K_{q_{mg_1\&ng_2\&(q-m-n)g_3}}$ of a three–dimensional conductance for $q \geq 2$ is given by

$$\frac{1}{m!n!(q-m-n)!}\frac{\partial i\left(v_i, v_j, v_k\right)}{\partial^m v_i \partial^n v_j \partial^{(q-m-n)} v_k} \quad (1)$$

  where g_1, g_2 and g_3 are the conductances through wich the current controlled by respectively v_i, v_j and v_k flows.
- The component of a signal at a frequency which is a linear combination of the input–signal frequencies, is denoted a *phasor*. E.g. the phasor $V_{(out,0),1,1}$ is the component of the signal $v_{out,0}$ at frequency $f_{in,1} + f_{in,2}$. The signal $v_{out,o}$ is re–constructed from all corresponding phasors using the formula

$$v_{(out,0)}(t) = \frac{1}{2}\sum_{m=-\infty}^{+\infty}\sum_{n=-\infty}^{+\infty} V_{(out,0),m,n} e^{j(m\omega_1+n\omega_2)t} \quad (2)$$

  with $\omega_x = 2\pi f_x$.

3 Algorithm

The algorithm used for analyzing weakly nonlinear circuits is explained in [6]. Only the conclusions are given here for reasons of brevity. There is one basic formula for calculating a phasor:

*Katholieke Universiteit Leuven, Dept. ESAT–MICAS, Kasteelpark Arenberg 10, B–3001 Leuven, Belgium {wim.verhaegen,georges.gielen}@esat.kuleuven.ac.be

$$V_{x,m,n} = \sum i_{NL} H_{i_{NL}\mapsto v_x}(mj\omega_1 + nj\omega_2) \quad (3)$$

with i_{NL} a fictitious current source, and $H_{i_{NL}\mapsto v_x}(s)$ a linear circuit function expressing the relation between the fictitious current and the entity of interest (in casu the voltage v_x). As is shown in [6], the fictitious current source is defined by the dimensionality of the associated conductance, and the values of the coefficients m and n, under the assumption that the circuit behaves in a weakly nonlinear way. E.g. the fictitious current source for a one–dimensional conductance and $m = 2$ and $n = -1$ is given by

$$K_{22_{g_1}}\left(V_{i,1,0}V_{i,1,-1} + V_{i,0,-1}V_{i,2,0}\right) + \tfrac{3}{4}K_{33_{g_1}}\, V_{i,1,0}^2 V_{i,0,-1} \quad (4)$$

Note that equation (4) refers to phasors of order 2, which can in turn be found using equation (3). These formulas are thus applied recursively, until an expression with linear phasors only — i.e. $(m, n) = (\pm 1, 0)$ or $(m, n) = (0, \pm 1)$ — is obtained.

The linear–analysis engine Symba is subsequently used to replace the linear transfer functions in the resulting expression with functions of the (linear) circuit elements. To this purpose, Symba internally uses a numerical approximation algorithm [7], and a matroid–based symbolic term generator [8] combined with an error controller.

The resulting expression with the linear circuit elements can grow quite large for circuits of low complexity already, but luckily many terms in it are negligible. The expression is therefore further simplified using a number of sorting and elimination techniques like numerical screening of the terms and adaptive control of the approximating linear analysis, controlled with the appropriate error algorithms. This finally results in an expression of the form (3), with a reduced number of terms.

Note, finally, that equation (3) yields an harmonic of a current or voltage. Many distortion specs — e.g. OIP2, IP3 — are expressed as a combination of several such components. For these cases we must repeat the nonlinear analysis process for the different components and combine the end results. An example of this will be given in section 4.

The repetitive application of equation (3) using nonlinearity stamps like the one in equation (4) has been automated in a nonlinear–analysis engine, which interacts with the user and the linear–analysis engine Symba. This engine has been implemented in Perl and C++ and is linked to the Symba linear–analysis engine. The use of the nonlinear–analysis engine on an example circuit is demonstrated in section 4.

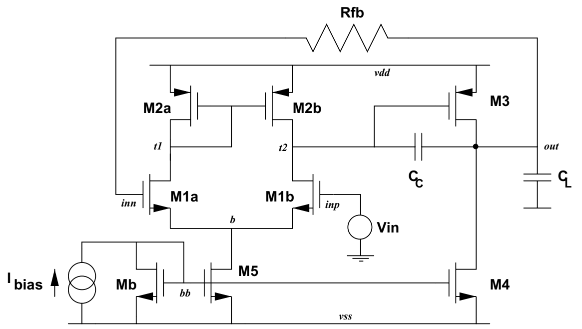

Figure 1: Schematic of the Miller opamp with feedback

4 Applications

The distortion in the Miller opamp shown in figure 1 is now analyzed as an illustration of the use of the nonlinear–analysis engine. The opamp has a differential input at the matched source–coupled pair M1a and M1b, and a single–ended output. The unity feedback obtained with the resistor Rfb configures the opamp as a voltage follower. The opamp has a gain–bandwidth product of 1 MHz, and we are interested in the second–order distortion below that frequency.

The application of all the fictitious current sources results in a second–order response at the output $V_{(out,0),2}$ which is the product of $\frac{v_{in}^2}{2}$ and the sum of contributions shown in table 1. The nonlinear coefficients K_* in the contributions are calculated as the derivatives of a transistor characteristic fitted through points obtained using a numerical simulator.

In order to interpret the expression for $V_{(out,0),2}$ and obtain an expression for, say, the second–order output–referred intermodulation product $OIP2$, the contributions (5) to (19) have to be further simplified. This is achieved in 4 subsequent steps:

1. The entries that contribute only a little to the value of $V_{(out,0),2}$ can be eliminated with a small loss of accuracy. This elimination needs to be validated over the entire frequency range of interest. In order to facilitate this, a relative weight is assigned to each entry using the following formula:

$$w_i(f) = \frac{|e_i(j\omega)|}{\left|V_{(out,0),2}(j\omega)\right|} \quad (20)$$

where $e_i(f)$ is the i'th entry as a function of the frequency. These weights are calculated based on the numerical reference value of the different terms, without any symbolic calculations.

Based on these weights, the entries (5) to (19) are examined for elimination in order of increasing maximum weight. The impact of the entries

$$K_{2_{gm\&go},M1B} H_{v_{inp,0} \mapsto v_{t2,b}}(j\omega)\, H_{v_{inp,0} \mapsto v_{inp,b}}(j\omega)\, H_{i_{DS,M1B} \mapsto v_{out,0}}(2j\omega) \tag{5}$$
$$K_{2_{gm\&go},M1A} H_{v_{inp,0} \mapsto v_{t1,b}}(j\omega)\, H_{v_{inp,0} \mapsto v_{inn,b}}(j\omega)\, H_{i_{DS,M1A} \mapsto v_{out,0}}(2j\omega) \tag{6}$$
$$K_{2_{2gm},M1B} H_{v_{inp,0} \mapsto v_{inp,b}}(j\omega)\, H_{v_{inp,0} \mapsto v_{inp,b}}(j\omega)\, H_{i_{DS,M1B} \mapsto v_{out,0}}(2j\omega) \tag{7}$$
$$K_{2_{2gm},M1A} H_{v_{inp,0} \mapsto v_{inn,b}}(j\omega)\, H_{v_{inp,0} \mapsto v_{inn,b}}(j\omega)\, H_{i_{DS,M1A} \mapsto v_{out,0}}(2j\omega) \tag{8}$$
$$\begin{gathered}(K_{2_{2go},M2A} + K_{2_{gm\&go},M2A} + K_{2_{2gm},M2A})* \\ H_{v_{inp,0} \mapsto v_{t1,vdd}}(j\omega)\, H_{v_{inp,0} \mapsto v_{t1,vdd}}(j\omega)\, H_{i_{DS,M2A} \mapsto v_{out,0}}(2j\omega)\end{gathered} \tag{9}$$
$$K_{2_{2gm},M2B} H_{v_{inp,0} \mapsto v_{t1,vdd}}(j\omega)\, H_{v_{inp,0} \mapsto v_{t1,vdd}}(j\omega)\, H_{i_{DS,M2B} \mapsto v_{out,0}}(2j\omega) \tag{10}$$
$$K_{2_{2gm},M3} H_{v_{inp,0} \mapsto v_{t2,vdd}}(j\omega)\, H_{v_{inp,0} \mapsto v_{t2,vdd}}(j\omega)\, H_{i_{DS,M3} \mapsto v_{out,0}}(2j\omega) \tag{11}$$
$$K_{2_{2go},M1B} H_{v_{inp,0} \mapsto v_{t2,b}}(j\omega)\, H_{v_{inp,0} \mapsto v_{t2,b}}(j\omega)\, H_{i_{DS,M1B} \mapsto v_{out,0}}(2j\omega) \tag{12}$$
$$K_{2_{2go},M1A} H_{v_{inp,0} \mapsto v_{t1,b}}(j\omega)\, H_{v_{inp,0} \mapsto v_{t1,b}}(j\omega)\, H_{i_{DS,M1A} \mapsto v_{out,0}}(2j\omega) \tag{13}$$
$$K_{2_{2go},M3} H_{v_{inp,0} \mapsto v_{out,vdd}}(j\omega)\, H_{v_{inp,0} \mapsto v_{out,vdd}}(j\omega)\, H_{i_{DS,M3} \mapsto v_{out,0}}(2j\omega) \tag{14}$$
$$K_{2_{2go},M4} H_{v_{inp,0} \mapsto v_{out,vss}}(j\omega)\, H_{v_{inp,0} \mapsto v_{out,vss}}(j\omega)\, H_{i_{DS,M4} \mapsto v_{out,0}}(2j\omega) \tag{15}$$
$$K_{2_{gm\&go},M3} H_{v_{inp,0} \mapsto v_{out,vdd}}(j\omega)\, H_{v_{inp,0} \mapsto v_{t2,vdd}}(j\omega)\, H_{i_{DS,M3} \mapsto v_{out,0}}(2j\omega) \tag{16}$$
$$K_{2_{2go},M5} H_{v_{inp,0} \mapsto v_{b,vss}}(j\omega)\, H_{v_{inp,0} \mapsto v_{b,vss}}(j\omega)\, H_{i_{DS,M5} \mapsto v_{out,0}}(2j\omega) \tag{17}$$
$$K_{2_{gm\&go},M2B} H_{v_{inp,0} \mapsto v_{t2,vdd}}(j\omega)\, H_{v_{inp,0} \mapsto v_{t1,vdd}}(j\omega)\, H_{i_{DS,M2B} \mapsto v_{out,0}}(2j\omega) \tag{18}$$
$$K_{2_{2go},M2B} H_{v_{inp,0} \mapsto v_{t2,vdd}}(j\omega)\, H_{v_{inp,0} \mapsto v_{t2,vdd}}(j\omega)\, H_{i_{DS,M2B} \mapsto v_{out,0}}(2j\omega) \tag{19}$$

Table 1: Contributions of all nonlinearities to $V_{(out,0),2}$ for the Miller opamp

on the total magnitude $\left|V_{(out,0),2}\right|$ — graphically illustrated in figure 2 — is used as a verification measure to accept or reject each elimination. It is found that (16) to (19) can safely be omitted. As a result of this step, no symbolic expressions will be generated for the omitted entries.

2. The transfer functions found in the contributions (5) through (15) are one by one approximated to obtain simple, interpretable expressions. The expressions are generated automatically using Symba, and can be approximated by very simple expressions due to the unity feedback.

3. After substitution of the simplified transfer function in the total distortion expression, it is found that all contributions (5) to (15) are paired, with the exception of (11). The thus paired contributions cancel in case the corresponding nonlinear coefficients are (approximately) equal. The differences between the (second–order) nonlinear coefficients are relatively larger than the differences between the (first–order) small–signal elements. It is thus logical to let the mismatch in the circuit be reflected through the former differences. The following contributions are thus found to be cancelling:

   - (5) and (6);
   - (7) and (8);
   - (9) and (10), taking into consideration that $K_{2_{2gm},M2a} \gg K_{2_{2go},M2a} + K_{2_{gm\&go},M2a}$;
   - and finally (14) and (15), although there is no fundamental reason for this. Note however that this coincidence does not really matter, as both contributions are negligible compared to entry (11) anyway.

   All these substitutions and eliminations finally result in the symbolic formula:

$$V_{(out,0),2} = \frac{v_{in}^2}{2}\left(-\frac{K_{2_{2gm},M3}}{g_{m_{M3}}} + \frac{K_{2_{2gm},M1b} - K_{2_{2gm},M1a}}{g_{m_{M1}}}\right) \tag{21}$$

4. Finally the output–referred second–order intercept point $OIP2$ is calculated, which is defined as the input amplitude for which $|V_{out}| = \left|V_{out,2}\right|$, i.e.

$$V_{out} = \frac{V_{out}^2}{2} \frac{\left|-g_{m_{M1}} K_{2_{2gm},M3} + g_{m_{M3}}\left(K_{2_{2gm},M1b} - K_{2_{2gm},M1a}\right)\right|}{g_{m_{M1}} g_{m_{M3}}} \tag{22}$$

   So $OIP2$ is given by

$$OIP2 = \frac{2 g_{m_{M1}} g_{m_{M3}}}{\left|-g_{m_{M1}} K_{2_{2gm},M3} + g_{m_{M3}}\left(K_{2_{2gm},M1b} - K_{2_{2gm},M1a}\right)\right|} \tag{23}$$

   For the design point chosen for the Miller opamp

$$2 g_{m_{M1}} g_{m_{M3}} = 824.5 \times 10^{-9} \tag{24}$$
$$-g_{m_{M1}} K_{2_{2gm},M3} = 424.11 \times 10^{-9} \tag{25}$$
$$g_{m_{M3}}\left(K_{2_{2gm},M1b} - K_{2_{2gm},M1a}\right) = -7.5656 \times 10^{-9} \tag{26}$$

   As a result the contribution of $K_{2_{2gm},M3}$ in the denominator of (23) is dominant, and the expression can be simplified to:

$$OIP2 = \left|\frac{2 g_{m_{M3}}}{K_{2_{2gm},M3}}\right| \tag{27}$$

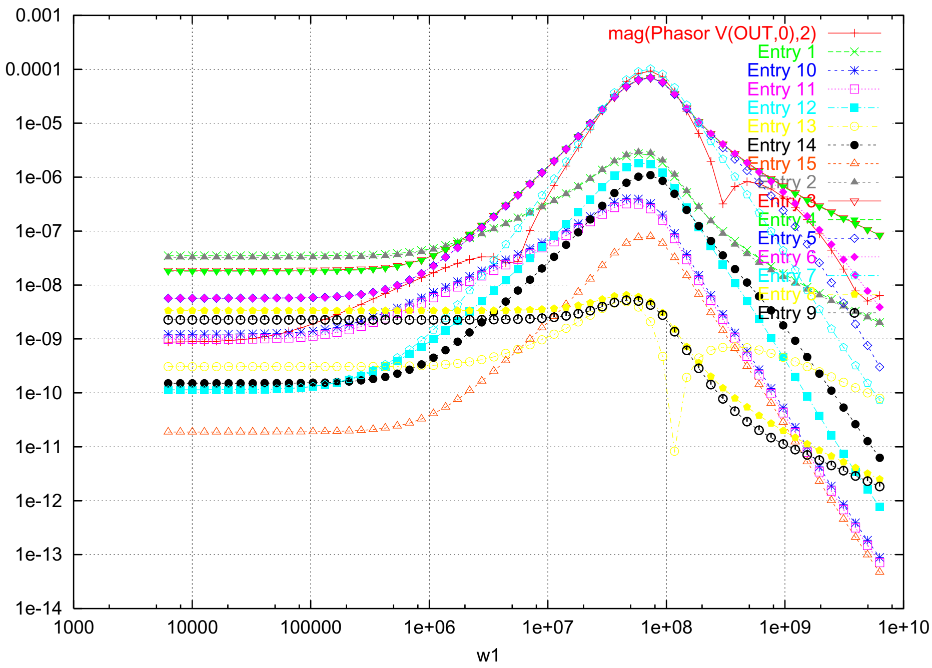

Figure 2: Frequency–dependent magnitudes of all contributions to, and the total phasor $V_{(out,0),2}$ for the Miller opamp

which equals 1.944V for the chosen design point.

Note that the obtained results are only valid in the case of perfectly matched transistor characteristics for the pairs M1a and M1b, resp. M2a and M2b. When this assumption cannot be made, the entire exercise needs to be repeated for the same circuit with mismatch introduced. This will of course result in a lower $OIP2$.

5 Conclusions

The extension of linear analysis to obtain closed–form symbolic expressions for the weakly nonlinear characteristics of analog integrated circuits has been demonstrated with an example circuit. The underlying algorithm and simplification of the lengthy results has been automated and linked to the existing Symba environment. The resulting simplified expressions can be used as design equations in an analog design framework.

Acknowledgments

This research has been funded in part by the Esprit project 21812 Amadeus.

References

[1] K. Kundert, J. White, and A. L. Sangiovanni-Vincentelli, *Steady–state methods for simulating analog and microwave circuits*. Kluwer Academic Publishers, 1990.

[2] J. Rowchowdhury, "MPDE methods for efficient analysis of wireless systems," in *Proceedings Custom Integrated Circuits Conference*, pp. 451–454, 1998.

[3] H. Floberg and S. Mattisson, "Symbolic distortion analysis of nonlinear elements in feedback amplifiers using describing functions," *Journal of Circuit Theory and Applications*, vol. 23, pp. 345–356, July 1995.

[4] W. Yu and B. H. Leung, "Distortion analysis of MOS track–and–hold sampling mixers using time–varying volterra series," *IEEE Transactions on Circuits and Systems–II: Analog and Digital Signal Processing*, vol. 46, pp. 101–113, Feb. 1999.

[5] W. Sansen, "Distortion in elementary transistor circuits," *IEEE Transactions on Circuits and Systems–II: Analog and Digital Signal Processing*, vol. 46, pp. 315–325, Mar. 1999.

[6] P. Wambacq, G. G. E. Gielen, P. R. Kinget, and W. Sansen, "High–frequency distortion analysis of analog integrated circuits," *IEEE Transactions on Circuits and Systems–II: Analog and Digital Signal Processing*, vol. 46, pp. 335–345, Mar. 1999.

[7] F. V. Fernández Fernandéz, O. Guerra, J. D. Rodríguez-García, and A. Rodríguez-Vázquez, "Corrections to symbolic analysis of large analog integrated circuits: The numerical reference generation problem," *IEEE Transactions on Circuits and Systems–II: Analog and Digital Signal Processing*, vol. 46, pp. 485–486, Apr. 1999.

[8] P. Dobrovolny, "Design tool for symbolic analysis based on the matroid intersection theory," in *Proceedings IEEE International Symposium on Circuits and Systems*, 1998.